Time-Resolved EPR and Transient Absorption Studies on Phthalocyaninatosilicon Covalently Linked to Two PROXYL Radicals

Shoji Takeuchi, Kazuyuki Ishii, and Nagao Kobayashi*

Department of Chemistry, Graduate School of Science, Tohoku University, Sendai 980-8578, Japan

Received: September 9, 2003; In Final Form: January 30, 2004

By the combined use of electron paramagnetic resonance (EPR) and transient absorption measurements, photophysical properties of tetra-*tert*-butylphthalocyaninatosilicon (SiPc) covalently linked to two 2,2,5,5-tetramethyl-1-pyrrolidinyloxy (PROXYL) radicals (R2a) have been investigated in terms of the photocontrol of magnetic properties. The steady-state EPR spectrum of R2a indicates that two PROXYL radicals generate a spin-correlated radical pair, where the singlet ground state (S_0') is close to the triplet ground state (T_0'). In time-resolved EPR (TREPR) spectra of R2a, *A*/*E A*/*E A*/*E* polarizations are initially seen, which then change into *E*/*A E*/*A E*/*A* polarizations. The initial and later polarizations are reproduced by spin-selective population of the S_0' and T_0' states, respectively. Quantitative analyses of TREPR and transient absorption signals show that the initial *A*/*E A*/*E A*/*E* polarizations are reproduced by spin-selective relaxation from the excited states, where the SiPc moiety is in the excited singlet state, and that the later *E*/*A E*/*A E*/*A* polarizations originate from the decay from excited multiplet states consisting of two doublet PROXYLs and SiPc in the excited triplet state.

Introduction

Interactions between photoexcited triplet molecules and paramagnetic species result in some important phenomena such as the quenching of photoexcited molecules[1,2] and the generation of excited singlet oxygen.[3] A time-resolved electron paramagnetic resonance (TREPR) method, which is a powerful technique for the observation of paramagnetic intermediates generated after photoexcitation, has been shown to be useful in investigating the interactions between photoexcited triplet molecules and stable radicals (e.g. electron-spin polarizations (ESPs) in radicals produced through interacting with excited triplet molecules[4,5] or the direct observation of excited multiplet states consisting of a photoexcited triplet chromophore and a doublet molecule.[6−9])

Recently, three-center four-spin (3c-4s) systems have generated considerable interest as a new area of excited multiplet study.[9−12] TREPR studies on the excited quintet states consisting of a photoexcited triplet chromophore and two doublet radicals have been carried out for the fullerene−nitroxides system by Yamauchi et al. and for the phenylanthoracene−iminonitroxides system by Teki et al..[9,10] However, photoinduced population transfer (PIPT) has been reported to be a new ESP in tetra-*tert*-butylphthalocyaninatosilicon (SiPc) covalently linked to two 2,2,6,6-tetramethyl-1-piperidinyloxy (TEMPO) radicals (R2c, Chart 1).[11] In the case of R2c, the two TEMPO radicals generate a spin-correlated radical pair, where the singlet ground state (S_0') is close to the triplet ground state (T_0'). In the TREPR spectrum in toluene solution, a triplet-precursor-type ESP was observed in the spin-correlated radical pair, which was reasonably interpreted by selective population from the excited multiplet states to the T_0' state. That is, the magnetic property in the ground state is changed before and after the photoexcitation, which was proposed as a novel concept for the photocontrol of magnetic properties. Corvaja et al. have investigated several fullerene bisadducts containing the nitroxide moiety, which also exhibit EPR spectra of spin-correlated radical pairs.[12] In the TREPR spectrum at ambient temperature, a singlet-precursor-type ESP was initially seen, which then changed into a triplet-precursor-type ESP. It was suggested that the initial singlet-precursor-type ESP could be interpreted by triplet−triplet interactions. Whereas these ESPs in the spin-correlated radical pairs are important not only for understanding the excited-state dynamics in radical−chromophore systems but also in terms of the photocontrol of the magnetic properties, the relationship between the two kinds of ESP behavior has not been examined experimentally and is therefore in need of clarification.

In this report, we have studied a novel derivative of SiPc covalently linked to two 2,2,5,5-tetramethyl-1-pyrrolidinyloxy (PROXYL) radicals (R2a, Chart 1), where the electron-exchange interaction between the SiPc and NR moieties is expected to be much larger than R2c[8] by the combined use of EPR and transient absorption measurements. The spin dynamics of R2a is investigated by quantitative analyses of the TREPR and transient absorption time profiles, and the relationship between the singlet-precursor-type and triplet-precursor-type ESPs is clarified.

Experimental Section

Materials. R2a was synthesized by analogy to R2c.[11] R0 (Chart 1) and 3-hydroxy-PROXYL were refluxed in toluene for 42 h.[8b] After neutral alumina and gel permeation (Bio-Beads S-x1 or S-x8, Bio-Rad) chromatography, R2a was isolated in 19% yield. UV−vis, ESI-TOF, and elemental analyses were satisfactory, as follows.

R2a: UV−vis (λ/nm ($\epsilon/10^4$)): 682.5 (26.0), 651.5 (3.45), 613.5 (4.19), 359.5 (8.69). ESI-TOF *m*/*e*: 1079 (M^+). Anal. Calcd for $C_{64}H_{78}N_{10}O_4Si$: C, 71.21; H, 7.28; N, 12.98. Found: C, 70.459; H, 7.402; N, 12.783.

Measurements. Spectral-grade toluene (Nacalai Tesque Inc.) was used as a solvent for all measurements. The concentrations

* To whom correspondence should be addressed. E-mail: nagaok@mail.tains.tohoku.ac.jp.

10.1021/jp036690l CCC: $27.50
Published on Web 03/26/2004

CHART 1

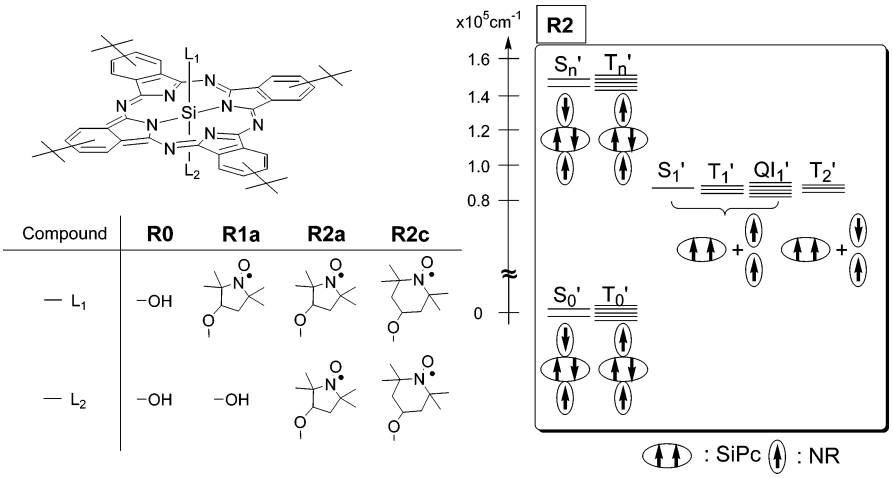

of the samples were $2 \times 10^{-5}-1 \times 10^{-3}$ M for transient absorption measurements and 1×10^{-3} M for TREPR measurements. For these time-resolved measurements, R2a was purified carefully before the measurements, samples were deaerated by freeze−pump−thaw cycles, and then the measurements were carried out within 2 days.

Steady-state UV−vis absorption spectra were measured with a Hitachi 330LC spectrometer. Steady-state fluorescence was recorded with a Hitachi F-4500 fluorescence spectrometer. Transient absorption measurements were performed at ambient temperature by using a monochromator (JASCO CT-25CP) and a photomultiplier (Hamamatsu Photonics R446) with the continuous wave of a metal halide lamp (Sigma Koki IMH-250) or a He−Ne green laser (543.5 nm, Melles Griot).[8b,11b] Samples were excited at 355 nm by a Nd:YAG laser (Spectra Physics INDI-30; 355 nm; 7 ns fwhm). The signals were integrated using a digital oscilloscope (Iwatsu-LeCroy LT342), where a 75-Ω resistance was employed for impedance matching, and thus the time-resolution of our instrument was ∼10 ns.[13] TREPR, pulse-EPR, and steady-state EPR measurements were carried out on a Bruker ESP 300E spectrometer.[7c,14] An Oxford ESR 900 cold gas flow system was used to control the temperature. For the TREPR measurements, samples were excited at 585 nm by a dye laser (Lumonics HD 500) pumped with an excimer laser (Lumonics EX 500, 13 ns fwhm), and the signals were integrated using a digital oscilloscope (Iwatsu-LeCroy LT342 or LeCroy 9450A).

Theoretical Background

To discuss the electron spin dynamics, we illustrate the electronic states of R2a (Chart 1). In the ground state, the S_0' and T_0' states are generated by two doublet PROXYLs (^{2}PROXYLs). The excited singlet (S_n') and triplet (T_n') states consist of two ^{2}PROXYLs and SiPc in the lowest excited singlet (S_1) state (^{1}SiPc*), which is almost entirely derived from the $^1(a_{1u}e_g)$ configuration. (The a_{1u} (π) and e_g (π^*) orbitals denote the HOMO and LUMO of the Pc ligand, respectively.) The electronic absorption spectrum of R2a indicates that ^{1}SiPc* is located at ∼14 700 cm^{-1}.[8,11,13]

However, interactions with SiPc in the lowest excited triplet (T_1) state (^{3}SiPc*) are complicated. The interactions between ^{3}SiPc* and two ^{2}PROXYLs result in the lowest excited singlet (S_1'), triplet (T_1'), and quintet (QI_1') states and the second-lowest excited triplet (T_2') state, where two ^{2}PROXYLs exhibit triplet and singlet character in the T_1' and T_2' states, respectively.[11b,15] Phosphorescence measurements indicate that ^{3}SiPc* originating from the $^3(a_{1u}e_g)$ configuration is located at 8900 cm^{-1}.[13] The electron exchange energies of the S_1', T_1', T_2', and QI_1' states are evaluated to be J, 0, $-J$, and $-2J$, respectively.[15]

Results and Interpretations

Steady-State EPR Measurements. Steady-state EPR spectra of R2a observed at 293 and 20 K are shown in Figure 1a and c, respectively. In the EPR spectrum at ambient temperature, new signals due to a spin-correlated radical pair consisting of PROXYL radicals are seen in addition to three signals that are due to the hyperfine coupling (hfc) of the nitrogen nucleus of PROXYL.[16] In this case, the spin Hamiltonian is represented as follows.[17]

$$H_{\text{spin}} = g\beta B(S_1 + S_2) + A_N(I_1S_1 + I_2S_2) - J'\left(2S_1S_2 + \frac{1}{2}\right) \quad (1)$$

A simulation spectrum calculated using eq 1 is shown in Figure 1b. The observed spectrum is well reproduced when the energy splitting ($2J'$) between the S_0' and T_0' states is 9.9×10^{-4} cm^{-1}

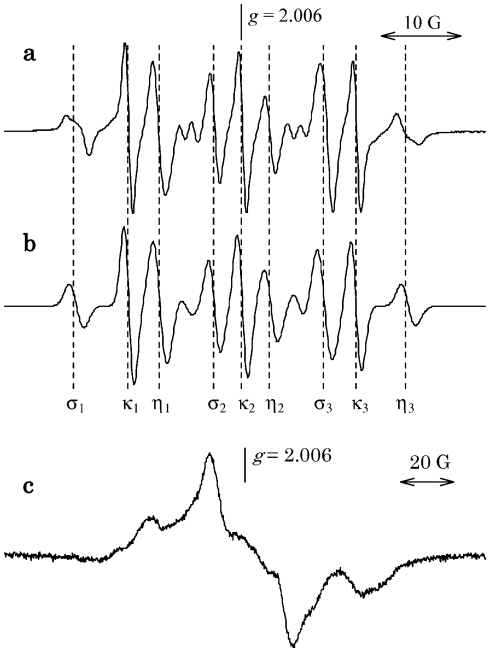

Figure 1. Steady-state EPR spectra of R2a (first derivative) at 293 K (a) and 20 K (c) with spectral simulation (b).

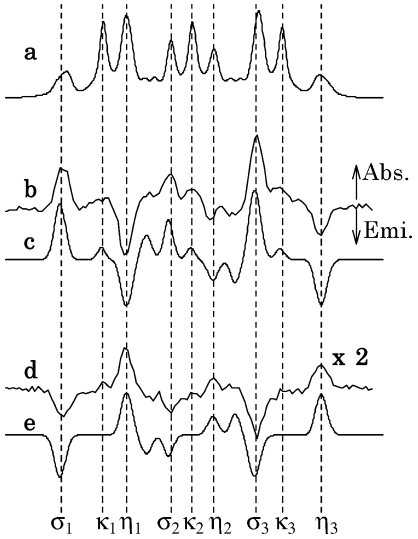

Figure 2. Steady-state absorption EPR spectrum (a) and TREPR spectra (b, d) of R2a with their spectral simulations (c, e). TREPR spectra were observed (b) 0.1 and (d) 0.5 μs after 585-nm laser excitation. Simulation spectra of c and e were calculated using $P(T_{0+}')$:$P(T_{00}')$:$P(S_0')$:$P(T_{0-}') = 0{:}0.1{:}0.8{:}0.1$ and $P(T_{0+}')$:$P(T_{00}')$:$P(S_0')$:$P(T_{0-}') = 0.33{:}0.33{:}0{:}0.33$, respectively.

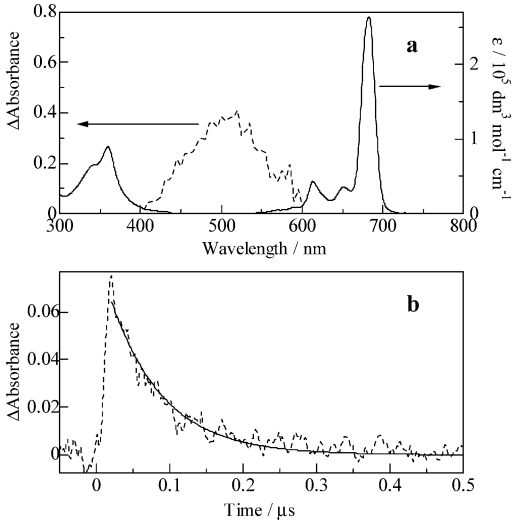

Figure 3. (a) Steady-state electronic absorption spectrum (—) and transient absorption spectrum (- - -) of R2a. The transient absorption spectrum was observed 25 ns after 355-nm laser excitation. (b) Transient absorption decay profile (- - -) of R2a measured at 543.5 nm. The fitting curve (—) was calculated by a least-squares method.

at ambient temperature, similar to that of R2c.[11] This spectrum is conveniently divided into two groups. One consists of κ_n signals ($n = 1-3$), which are transitions when $m_{N1} = m_{N2}$, where m_{Ni} ($i = 1, 2$) is the magnetic quantum number of nitrogen nucleus i. The eigenfunctions are represented as $|T_{0+}'\rangle$, $|T_{00}'\rangle$, $|S_0'\rangle$, and $|T_{0-}'\rangle$ without S−T_0 mixing.[18] The other consists of σ_n and η_n signals, which are transitions that occur when $m_{N1} \neq m_{N2}$. The eigenfunctions are $|T_{0+}'\rangle$, $|T_{0-}'\rangle$, $|\Psi_1'\rangle$ (= cos θ $|S_0'\rangle$ + sin θ $|T_{00}'\rangle$, tan $2\theta = \langle S_0'|H_{spin}|T_{00}'\rangle/J'$), and $|\Psi_2'\rangle$ (= − sin θ $|S_0'\rangle$ + cos θ $|T_{00}'\rangle$) with S−T_0 mixing.

The EPR spectrum at 20 K exhibits a typical triplet EPR spectrum, in contrast to that for R2c.[7f] From the spectral splitting, the zero-field splitting parameter D value was evaluated to be ~40 G. Because the $|D|$ value can be approximated as $2.80 \times 10^4 R^{-3}$ (R denotes the average distance between triplet spins),[19] the R value of R2a was evaluated to be 11 Å. This is consistent with the structure optimized by the MM+ calculations,[20] where the distances between the two nitroxide nitrogens and between the two nitroxide oxygens are 10.1 and 12.3 Å, respectively.

TREPR Measurements. TREPR spectra of R2a observed at 0.1 and 0.5 μs are shown in Figure 2b and d, respectively.[9] *A/E A/E A/E* signals are initially seen at 0.1 μs, changing into *E/A E/A E/A* ESPs at 0.5 μs. The initial *A/E A/E A/E* polarizations correspond to the singlet-precursor-type ESP of the spin-correlated radical pair and were reproduced using $P(T_{0+}')$:$P(T_{00}')$:$P(S_0')$:$P(T_{0-}') = 0{:}0.1{:}0.8{:}0.1$.[21,22] The *E/A E/A E/A* polarizations correspond to the triplet-precursor-type ESP and were interpreted by selective population of the T_0' state (i.e., $P(T_{0+}')$:$P(T_{00}')$:$P(S_0')$:$P(T_{0-}') = 0.33{:}0.33{:}0{:}0.33$). [22] The *E/A E/A E/A* polarizations are similar to those of R2c,[11] and the polarization inversion from *A/E A/E A/E* to *E/A E/A E/A* is similar to that seen for fullerene bisadducts containing the nitroxide moiety.[12]

Fluorescence and Transient Absorption Measurements. A steady-state electronic absorption spectrum of R2a is shown in Figure 3a. The electronic absorption spectrum is independent of the substitution of PROXYL radicals, indicating that the electronic interaction between the excited singlet SiPc and ^{2}PROXYLs is very weak.[8b] Although the fluorescence spectrum was unchanged by the PROXYL substitution, the fluorescence quantum yield (0.0036) of R2a determined by the use of R0 (0.57) was much smaller than those of R0 and R1a (= 0.16).[8] This originates from the intersystem crossing (ISC) enhancement, resulting from transitions between states having the same spin multiplicity (i.e., $S_n' \rightarrow S_1'$, $T_n' \rightarrow T_1'$, and $T_n' \rightarrow T_2'$).

To investigate ^{3}SiPc*, transient absorption measurements were carried out for R2a. A transient absorption spectrum and the decay profile of R2a are shown in Figure 3a and b, respectively. The spectrum is very similar to triplet−triplet absorption spectra of Pc derivatives,[8b,11b] indicating that the electronic interaction between the excited triplet SiPc and ^{2}PROXYLs is small. The transient absorption decay was analyzed with a single-exponential function. The lifetime of R2a was evaluated to be 70 ± 20 ns,[23] which is much shorter than that (3.7 μs) of R2c,[11] reflecting the fact that the electron exchange interaction between the SiPc and PROXYL moieties is larger than that between the SiPc and TEMPO moieties.

Discussion

In the case of R2a, *A/E A/E A/E* ESPs corresponding to the singlet-precursor type are initially seen, which then change into the *E/A E/A E/A* ESPs of the triplet-precursor type. As shown in Figure 4a, the time-profile of the σ_1 signal clearly demonstrates that a new *E* polarization is generated after the decay of the first *A* polarization. This ESP inversion is similar to that of fullerene derivatives[12] and the first example in porphyrinic compounds.[11] In the following text, we will try to clarify these spin dynamics quantitatively.

Because the population of the $|\Psi_i'\rangle$ state ($i = 1, 2$) is represented by $\rho(i)[S_0'] + (1 - \rho(i))[T_{00}']$ ($\rho(i) = i - 1 + (-)^{i-1} \cos^2 \theta$), the σ_1 signal intensity, originating from the difference between the $|T_{0j}'\rangle$ (j = + or −) and $|\Psi_i'\rangle$ states, is represented as follows.

$$[\Psi_i'] - [T_{0j}'] = \rho(i)[S_0'] + (1 - \rho(i))[T_{00}'] - [T_{0j}']$$
$$= \rho(i)\left([S_0'] - \frac{[T_0']}{3}\right) \quad (2)$$

Here, it is assumed that $[T_{0+}'] = [T_{00}'] = [T_{0-}'] = [T_0']/3$

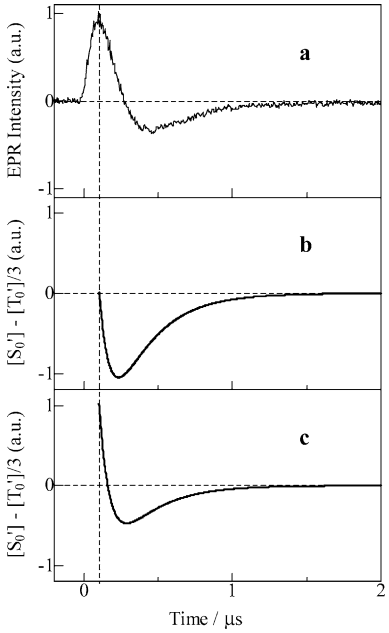

Figure 4. Time profile (a) of the σ_1 TREPR signal with the calculated time profiles of ($[S_0'] - ([T_0']/3)$) (b, c). Time profiles of ($[S_0'] - ([T_0']/3)$) were calculated in terms of the fourth-order Runge−Kutta method using $k_1 = k_2 = 9.0 \times 10^7\ s^{-1}$, $k_3 = k_4 = 2.4 \times 10^7\ s^{-1}$, and $k_5 = 9.6 \times 10^5\ s^{-1}$, respectively, and the α values were 1000 ($[S_1']_0 = 0.25$, $[T_1' + T_2']_0 = 0.75$, and $[QI_1']_0 = [S_0']_0 = [T_0']_0 = 0$) and 0.6 for time profiles b and c, respectively.

because κ_n signals exhibit no ESP. Thus, the EPR intensity of the σ_1 signal is proportional to $[S_0'] - ([T_0']/3)$. After the complete relaxation from S_n' and T_n' states within the time resolution of our TREPR instruments (∼100 ns), the differential equations of S_1', $T_1' + T_2'$, QI_1', S_0', and T_0' states are represented using Scheme 1 as follows.

$$\frac{d[S_1']}{dt} = -(6k_1 + k_3)[S_1'] + k_1[T_1' + T_2'] \qquad (3a)$$

$$\frac{d[T_1' + T_2']}{dt} = 6k_1[S_1'] - (k_1 + 5k_2 + k_4)[T_1' + T_2'] + 6k_2[QI_1'] \qquad (3b)$$

$$\frac{d[QI_1']}{dt} = 5k_2[T_1' + T_2'] - 6k_2[QI_1'] \qquad (3c)$$

$$\frac{d[S_0']}{dt} = k_3[S_1'] - 3k_5[S_0'] + k_5[T_0'] \qquad (3d)$$

$$\frac{d[T_0']}{dt} = k_4[T_1' + T_2'] + 3k_5[S_0'] - k_5[T_0'] \qquad (3e)$$

Here, $[T_1']$ and $[T_2']$ are summarized because the internal conversion between the T_1' and T_2' states should be very fast. These simultaneous differential equations were analyzed by the fourth-order Runge−Kutta method, from which the population difference between the S_0' and T_0' states was evaluated.

Initially, the ESPs due to the decay from ^{3}SiPc* (i.e., the S_1', T_1', T_2' and QI_1' states) are discussed by assuming that the initial populations, $[S_1']_0$, $[T_1' + T_2']_0$, $[QI_1']_0$, $[S_0']_0$, and $[T_0']_0$, are 0.25, 0.75, 0, 0, and 0, respectively. From transient absorption measurements carried out under the same experimental conditions as those used for the TREPR measurements ([R2a] = 10^{-3} M, 3300 G), the excited-state lifetime of R2a

SCHEME 1

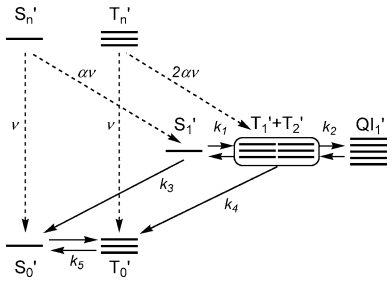

($= 1/k_M'$) was evaluated to be 70 ns.[23] When k_1 ($= k_2$) ≫ k_3 ($= k_4$), the k_3 value was estimated to be $2.4 \times 10^7\ s^{-1}$ using $k_M' \approx 7k_3/12$.[11b] In addition, the spin−lattice relaxation (SLR) time of the σ_1 signal was evaluated to be 0.52 μs by the inversion recovery measurement,[24] from which the k_5 value was estimated to be $9.6 \times 10^5\ s^{-1}$. A time profile calculated using these values is shown in Figure 4b.[25] The initial *A* polarization of the singlet-precursor type could not be seen, in contrast to the later *E* polarization of the triplet-precursor type. That is, the singlet-precursor-type polarization cannot be reproduced only by the relaxation from ^{3}SiPc* (i.e., the S_1', T_1', T_2', and QI_1' states), whereas the triplet-precursor-type polarization is interpreted by the fact that the decays from the T_1', T_2', and QI_1' states to the T_0' state are faster than those to the S_0' state because of the smaller change in the spin quantum number.[11]

Thus, the relaxation from ^{1}SiPc* (i.e., the S_n' and T_n' states) should be considered. From the S_n' state, the transition to the S_0' state (^{1}SiPc* → ^{1}SiPc internal conversion, IC) competes with that to the S_1' state (^{1}SiPc* → ^{3}SiPc* intersystem crossing, ISC). However, in the case of the T_n' state, the ^{1}SiPc* → ^{3}SiPc* ISC is preferable to that of the S_n' state because the interactions between ^{3}SiPc* and two ^{2}PROXYLs produce two triplet states, T_1' and T_2'. When the ^{1}SiPc* → ^{3}SiPc* ISC rate constant is α times the ^{1}SiPc* → ^{1}SiPc IC rate constant ($= \nu$), the initial populations after the relaxation from the S_n' and T_n' states were calculated as follows.

$$[S_1']_0 = \left(\frac{1}{4}\right) \times \left\{\frac{\alpha\nu}{\nu + \alpha\nu}\right\} = \frac{\alpha}{4 + 4\alpha} \qquad (4a)$$

$$[T_1' + T_2']_0 = \left(\frac{3}{4}\right) \times \left\{\frac{2\alpha\nu}{\nu + 2\alpha\nu}\right\} = \frac{3\alpha}{2 + 4\alpha} \qquad (4b)$$

$$[QI_1']_0 = 0 \qquad (4c)$$

$$[S_0']_0 = \left(\frac{1}{4}\right) \times \left\{\frac{\nu}{\nu + \alpha\nu}\right\} = \frac{1}{4 + 4\alpha} \qquad (4d)$$

$$[T_0']_0 = \left(\frac{3}{4}\right) \times \left\{\frac{\nu}{\nu + 2\alpha\nu}\right\} = \frac{3}{4 + 8\alpha} \qquad (4e)$$

The time profile calculated using $\alpha = 0.6$ is shown in Figure 4c.[25,26] The initial *A* polarization is 2 times the later *E* polarization, which reproduces the experimental trend. Thus, the initial singlet-precursor-type ESP originates mainly from the spin-selective relaxation from ^{1}SiPc* (i.e., the S_n' and T_n' states).[27]

Conclusions

We have studied a derivative of SiPc covalently linked to two PROXYL radicals, R2a, by the combined use of TREPR and transient absorption measurements. Quantitative analyses of the TREPR time profile have shown that the initial singlet-precursor-type ESP originates mainly from the spin-selective

decay from ^{1}SiPc* (i.e., the S_n' and T_n' states) and that the later triplet-precursor-type ESP can be interpreted by the spin-selective decay from ^{3}SiPc* (i.e., the S_1', T_1', T_2', and QI_1' states). That is, the magnetic properties in the ground state are varied by photoexcitation, as follows.

$$[S_0'] \approx \frac{[T_0']}{3} \xrightarrow{h\nu} [S_0'] > \frac{[T_0']}{3} \rightarrow [S_0'] < \frac{[T_0']}{3} \xrightarrow{SLR} [S_0'] \approx \frac{[T_0']}{3} \quad (5)$$

As shown in eq 5, this study demonstrates a novel PIPT between the S_0' and T_0' states, but it is very difficult to change the difference between the S_0' and T_0' states by varying the temperature when $|2J'| \approx 10^{-3}$ cm^{-1}. Therefore, our analysis is useful for the photocontrol of magnetic properties in the radical−chromophore system.

Acknowledgment. This work was partially carried out in the Advanced Instrumental Laboratory for Graduate Research of the Department of Chemistry, Graduate School of Science, Tohoku University, and was supported by a Grant-in-Aid for Young Scientists (category A no. 14703007), Scientific Research in Priority Areas "Diagnosis and Treatment of Cancer" (no. 15025212), and the COE project, Giant Molecules and Complex Systems, 2003 from the Ministry of Education, Culture, Sports, Science and Technology, Japan.

References and Notes

(1) (a) Kuzmin, V. A.; Tatikolov, A. S.; Borisevich, Yu. E. *Chem. Phys. Lett.* **1978**, *53*, 52. (b) Kuzmin, V. A.; Tatikolov, A. S. *Chem. Phys. Lett.* **1978**, *53*, 606. (c) Watkins, A. R. *Chem. Phys. Lett.* **1980**, *70*, 262. (d) Schwerzel, R. E.; Caldwell, R. A. *J. Am. Chem. Soc.* **1973**, *95*, 1382. (e) Caldwell, R. A.; Schwerzel, R. E. *J. Am. Chem. Soc.* **1972**, *94*, 1035. (f) Chattopadhyay, S. K.; Das, P. K.; Hug, G. L. *J. Am. Chem. Soc.* **1983**, *105*, 6205. (g) Watkins, A. R. *Chem. Phys. Lett.* **1974**, *29*, 526. (h) Green, J. A., II; Singer, L. A.; Parks, J. H. *J. Chem. Phys.* **1973**, *58*, 2690. (i) Green, J. A., II; Singer, L. A. *J. Am. Chem. Soc.* **1974**, *96*, 2730.

(2) (a) Gouterman, M. In *The Porphyrins*; Dolphin, D., Ed.; Academic: New York, 1978; Vol. 3, pp 1−165. (b) Ferraudi, G. In *Phthalocyanines: Properties and Applications*; Leznoff, C. C., Lever, A. B. P., Eds.; VCH Publishers: New York, 1989; Vol. 1, pp 291−340.

(3) (a) Porter, G.; Wright, M. R. *Discuss. Faraday Soc.* **1959**, *27*, 18. (b) Hoytink, G. J. *Acc. Chem. Res.* **1969**, *2*, 114. (c) Gijzeman, O. L. J.; Kaufman, F.; Porter, G. *J. Chem. Soc., Faraday Trans. 2* **1973**, *69*, 708. (d) Rosenthal, I.; Ben-Hur, E. In *Phthalocyanines: Properties and Applications*; Leznoff, C. C., Lever, A. B. P., Eds.; VCH Publishers: New York, 1989; Vol. 1, pp 393−425. (e) Rosenthal, I. In *Phthalocyanines: Properties and Applications*; Leznoff, C. C., Lever, A. B. P., Eds.; VCH Publishers: New York, 1996; Vol. 4, pp 481−514, and many references therein.

(4) (a) Blättler, C.; Jent, F.; Paul, H. *Chem. Phys. Lett.* **1990**, *166*, 375. (b) Kawai, A.; Okutsu, T.; Obi, K. *J. Phys. Chem.* **1991**, *95*, 9130. (c) Kawai, A.; Obi, K. *J. Phys. Chem.* **1992**, *96*, 52. (d) Kawai, A.; Obi, K. *Res. Chem. Intermed.* **1993**, *19*, 865. (e) Turro, N. J.; Khudyakov, I. V.; Bossmann, S. H.; Dwyer, D. W. *J. Phys. Chem.* **1993**, *97*, 1138. (f) Jockusch, S.; Dedola, G.; Lem, G.; Turro, N. J. *J. Phys. Chem. B* **1999**, *103*, 9126. (g) Corvaja, C.; Franco, L.; Pasimeni, L.; Toffoletti, A.; Montanari, L. *Chem. Phys. Lett.* **1993**, *210*, 355. (h) Corvaja, C.; Franco, L.; Toffoletti, A. *Appl. Magn. Reson.* **1994**, *7*, 257. (i) Corvaja, C.; Franco, L. Pasimeni, L.; Toffoletti, A. *J. Chem. Soc., Faraday Trans.* **1994**, *90*, 3267. (j) Hugerat, M.; van der Est, A.; Ojadi, E.; Biczok, L.; Linschitz, H.; Levanon, H.; Stehlik, D. *J. Phys. Chem.* **1996**, *100*, 495. (k) Regev, A.; Galili, T.; Levanon, H. *J. Phys. Chem.* **1996**, *100*, 18502.

(5) (a) Fujisawa, J.; Ishii, K.; Ohba, Y.; Iwaizumi, M.; Yamauchi, S. *J. Phys. Chem.* **1995**, *99*, 17082. (b) Fujisawa, J.; Ohba, Y.; Yamauchi, S. *J. Phys. Chem. A* **1997**, *101*, 434. (c) Jenks, W. S.; Turro, N. J. *Res. Chem. Intermed.* **1990**, *13*, 237.

(6) (a) Corvaja, C.; Maggini, M.; Prato, M.; Scorrano, G.; Venzin, M. *J. Am. Chem. Soc.* **1995**, *117*, 8857. (b) Corvaja, C.; Maggini, M.; Ruzzi, M.; Scorrano, G.; Toffoletti, A. *Appl. Magn. Reson.* **1997**, *12*, 477. (c) Mizuochi, N.; Ohba, Y.; Yamauchi, S. *J. Phys. Chem. A* **1997**, *101*, 5966. (d) Mizuochi, N.; Ohba, Y.; Yamauchi, S. *J. Phys. Chem. A* **1999**, *103*, 7749.

(7) (a) Ishii, K.; Fujisawa, J.; Ohba, Y.; Yamauchi, S. *J. Am. Chem. Soc.* **1996**, *118*, 13079. (b) Fujisawa, J.; Ishii, K.; Ohba, Y.; Yamauchi, S.; Fuhs, M.; Möbius, K. *J. Phys. Chem. A* **1997**, *101*, 5869. (c) Ishii, K.; Fujisawa, J.; Adachi, A.; Yamauchi, S.; Kobayashi, N. *J. Am. Chem. Soc.* **1998**, *120*, 3152. (d) Fujisawa, J.; Ishii, K.; Ohba, Y.; Yamauchi, S.; Fuhs, M.; Möbius, K. *J. Phys. Chem. A* **1999**, *103*, 213. (e) Ishii, K.; Ishizaki, T.; Kobayashi, N. *J. Phys. Chem. A* **1999**, *103*, 6060. (f) Ishii, K.; Kobayashi, N. *Coord. Chem. Rev.* **2000**, *198*, 231. (g) Ishii, K.; Ishizaki, T.; Kobayashi, N. *J. Chem. Soc., Dalton Trans.* **2001**, 3227. (h) Ishii, K.; Ishizaki, T.; Kobayashi, N. *Chem. Lett.* **2001**, 482. (i) Ishii, K.; Bottle, S. E.; Shimizu, S.; Smith, C. D.; Kobayashi, N. *Chem. Phys. Lett.* **2003**, *370*, 94. (j) Ishii, K.; Ishizaki, T.; Kobayashi, N. *Appl. Magn. Reson.* **2003**, *23*, 369.

(8) (a) Ishii, K.; Hirose, Y.; Kobayashi, N. *J. Phys. Chem. A* **1999**, *103*, 1986. (b) Ishii, K.; Takeuchi, S.; Kobayashi, N. *J. Phys. Chem. A* **2001**, *105*, 6794. (c) Ishii, K.; Hirose, Y.; Kobayashi, N. *J. Porphyrins Phthalocyanines* **1999**, *3*, 439.

(9) (a) Teki, Y.; Miyamoto, S.; Iimura, K.; Nakatsuji, M.; Miura, Y. *J. Am. Chem. Soc.* **2000**, *122*, 984. (b) Teki, Y.; Miyamoto, S.; Nakatsuji, M.; Miura, Y. *J. Am. Chem. Soc.* **2001**, *123*, 294.

(10) (a) Mizuochi, N.; Ohba, Y.; Yamauchi, S. *J. Chem. Phys.* **1999**, *111*, 3479. (b) Conti, F.; Corvaja, C.; Toffoletti, A.; Mizuochi, N.; Ohba, Y.; Yamauchi, S.; Maggini, M. *J. Phys. Chem. A* **2000**, *104*, 4962.

(11) (a) Ishii, K.; Hirose, Y.; Kobayashi, N. *J. Am. Chem. Soc.* **1998**, *120*, 10551. (b) Ishii, K.; Hirose, Y.; Fujitsuka, M.; Ito, O.; Kobayashi, N. *J. Am. Chem. Soc.* **2001**, *123*, 702.

(12) (a) Corvaja, C.; Franco, L.; Mazzoni, M.; Maggini, M.; Zordan, G.; Menna, E.; Scorrano, G. *Chem. Phys. Lett.* **2000**, *330*, 287. (b) Corvaja, C.; Franco, L.; Mazzoni, M. *Appl. Magn. Reson.* **2001**, *20*, 71.

(13) Ishii, K.; Takeuchi, S.; Shimizu, S.; Kobayashi, N. *J. Am. Chem. Soc.* **2004**, *126*, 2082.

(14) Fukuju, T.; Yashiro, H.; Maeda, K.; Murai, H. *Chem. Phys. Lett.* **1999**, *304*, 173.

(15) (a) Bencini, A.; Gatteschi, D. *EPR of Exchange Coupled Systems*; Springer-Verlag: Berlin, 1990. (b) Kahn, O. *Molecular Magnetism*; Wiley-VCH: New York, 1993.

(16) (a) Glarum, S. H.; Marshall, J. H. *J. Chem. Phys.* **1967**, *47*, 1374. (b) Nakajima, A.; Ohya-Nishiguchi, H.; Deguchi, Y. *Bull. Chem. Soc. Jpn.* **1972**, *45*, 713.

(17) g is the g factor of the electron; S_1 and S_2 are the electron spin operators of electrons 1 and 2, respectively; I_1 and I_2 are the nuclear spin operators of nitrogen nuclei 1 and 2, respectively; B is the external static magnetic field; β is the Bohr magneton; A_N is the hfc constant of the nitrogen nucleus; and $2J'$ is the singlet−triplet splitting.

(18) $|T_{0+}'\rangle = |\alpha\alpha\rangle$, $|T_{00}'\rangle = 2^{-1/2}(|\alpha\beta\rangle + |\beta\alpha\rangle)$, $|S_0'\rangle = 2^{-1/2}(|\alpha\beta\rangle - |\beta\alpha\rangle)$, $|T_{0-}'\rangle = |\beta\beta\rangle$

(19) Kuwata, K.; Ito, K. *Primer of Electron Spin Resonance*; Nankodo: Tokyo, 1980 (in Japanese).

(20) MM+ calculations were carried out by means of the program *Hyper Chem R. 5.1*; Hypercube Inc.: Gainesville, FL, 1998.

(21) The sign of the J' value was assumed to be negative: Adrian, F. J. *Rev. Chem. Intermed.* **1979**, *3*, 3.

(22) (a) Sakaguchi, Y.; Hayashi, H.; Murai, H.; I'Haya, Y. J. *Chem. Phys. Lett.* **1984**, *110*, 275. (b) Sakaguchi, Y.; Hayashi, H.; Murai, H.; I'Haya, Y. J.; Mochida, K. *Chem. Phys. Lett.* **1985**, *120*, 401. (c) Buckley, C. D.; Hunter, D. A.; Hore, P. J.; McLauchlan, K. A. *Chem. Phys. Lett.* **1987**, *135*, 307. (d) Tominaga, K.; Yamauchi, S.; Hirota, N. *J. Chem. Phys.* **1990**, *92*, 5175.

(23) The short excited-state lifetime of R2a was independent of concentrations or magnetic field.

(24) The inversion recovery method was carried out using a $\pi - \pi/2$ pulse sequence.

(25) In these calculations, we employed $k_1 (= k_2) = 9 \times 10^8$ s^{-1} because the transient absorption decay was analyzed with a single-exponential function.

(26) When $\alpha = 0.6$, the quantum yield of ^{3}SiPc* ($= [S_1']_0 + [T_1' + T_2']_0 = \alpha/(4 + 4\alpha) + 3\alpha/(2 + 2\alpha)$) is ∼0.5, which is close to those (0.54−0.67) of the NR−SiPc system reported previously.[13]

(27) In the case of R2c, the singlet-precursor-type ESP was not observed because it competes with the E polarizations generated in the excited multiplet states.